Available online at www.sciencedirect.com
SCIENCE DIRECT®
Journal of Power Sources 130 (2004) 77–84
JOURNAL OF POWER SOURCES
www.elsevier.com/locate/jpowsour

Methane to syngas conversion Part I. Equilibrium conditions and stability requirements of membrane materials

J.R. Frade*, V.V. Kharton, A. Yaremchenko, E. Naumovich

Ceramics and Glass Engineering Department (CICECO), University of Aveiro, 3810-193 Aveiro, Portugal

Received 8 July 2003; accepted 24 November 2003

Abstract

Thermodynamic data have been used to predict the dependence of methane conversion on temperature and oxygen partial pressure in mixed conducting membrane reactors, and the corresponding fractions of water vapor, H_2, CO and CO_2. The relations between methane conversion, gas composition and oxygen partial pressure were also used to formulate the oxygen balance in mixed conducting membrane reactors, with tubular reactor and continuous stirred tank reactor (CSTR) configurations. A single dimensionless parameter accounts for the combined effects of geometric parameters of the membrane reactor, the permeability of the membrane material, and flow rate at the entry of the reactor. Selected examples were calculated to illustrate the effects of steam to methane and inert to methane ratios in the gas entering the reactor. The values of oxygen partial pressure required to attain the highest yield of CO and H_2 were also used to estimate the stability requirements to be met by mixed conducting membrane materials. Suitable membrane designs might be needed to bridge the difference between the conditions inside the reactors and the stability limits of known mixed conductors.

Keywords: Cracking; Equilibrium; Syngas

1. Introduction

Methane is the main component of natural gas and biogas. It is thus a very important energy source and it might also be converted to a variety of useful chemicals. However, the efficiency of the actual energy conversion methods is relatively low, and excessive production of CO_2 is contributing to global warming. New energy conversion systems (e.g. fuel cells) are thus needed. Unfortunately, these alternative systems are still ill-suited to allow the direct conversion of hydrocarbons in fuel cells, thus requiring previous reforming, or conversion to syngas, i.e. a mixture of H_2 and CO.

Methane can be converted by partial oxidation when oxygen is provided by transport through a mixed conducting membrane [1–9], or through an ionic conductor with electronic short-circuiting or assisted by electrochemical pumping [10]. The mixed conducting membrane technology should integrate controlled oxygen separation, steam- or CO_2-reforming, and partial oxidation in a single step [1]. The technology has also a potential for energy and cost reduction, as well as reduction of NO_x emissions. Thus, new mixed conducting materials are still being studied [11–19].

Under suitable operating conditions one seeks the following reaction:

$$CH_4 + \tfrac{1}{2}O_2 \Leftrightarrow CO + 2H_2 \quad (1)$$

However, equilibrium is unlikely to be attained easily, and one may need to resort to somewhat excessive oxygen partial pressure to attain high conversion of methane, thus running risks of further oxidation of the components of the syngas mixture to water vapor and/or carbon dioxide, as follows:

$$CO + \tfrac{1}{2}O_2 \Leftrightarrow CO_2 \quad (2)$$

$$H_2 + \tfrac{1}{2}O_2 \Leftrightarrow H_2O \quad (3)$$

Under real conditions one should also consider the effects of methane cracking $CH_4 \rightarrow C+2H_2$, especially on contacting metallic surfaces (e.g. Ni or Fe); this shortcoming is one of the main limitations of the Ni/YSZ cermet anodes of solid oxide fuel cells, and explains the search for alternative SOFC anode materials for direct conversion of hydrocarbons [20–22]. Copper is one of the rare exceptions of metals with low activity towards methane cracking, and has been proposed for some of these concepts [22].

* Corresponding author. Tel.: +351-234370254; fax: +351-234425300.
E-mail address: jfrade@cv.ua.pt (J.R. Frade).

0378-7753/$ – see front matter © 2004 Elsevier B.V. All rights reserved.
doi:10.1016/j.jpowsour.2003.11.067

The main complications resulting from methane cracking in electrochemical systems is carbon deposition, thus blocking the methane conversion systems, and indeed causing a decrease in efficiency, because CO can be valuable as an important contribution of the total energy supply, and/or for the production of chemicals. Cracking may be somewhat minimized by avoiding metallic surfaces, i.e. by using all ceramic systems, such as mixed conducting ceramic membranes, and by ensuring conditions when partial oxidation and steam reforming of methane are more favorable. To minimize the risks of methane cracking one should thus avoid the use of metallic surfaces at high temperatures, when cracking is thermodynamically feasible. Ceramic mixed conducting membranes are expected to be more promising than ionic conductors with metallic electrodes for electrochemical pumping or short-circuited. One should also attempt to enhance the kinetics of reactions of partial oxidation and steam reforming.

Though the highest permeability was reported for perovskite materials, such as (La,Sr)(Co,Fe)$O_{3-\delta}$ [1,2], or related structures (e.g. La_2NiO_4) [17–19], these materials show some critical limitations, mainly in what concerns the limited chemical stability and decrease in permeability under reducing conditions, significant lattice expansion under high gradients of oxygen chemical potential, excessive thermal expansion, and possibly also reaction with CO_2. $LaMnO_3$- and $LaCrOO_3$-based materials possess higher stability but their permeability is poor. Mixed titanate–ferrate compositions [9,11–13] are among the most promising materials to meet the requirements of permeability, stability and low price.

A detailed knowledge of the conditions required for operation of mixed conducting membrane reactions is thus needed for the selection of materials, reactor configurations, and to optimize the operating conditions in terms of methane conversion, selectivity of reaction products, and stability of the mixed conducting membranes.

2. Gas composition assuming equilibrium without cracking

One may thus estimate the changes in gas composition for this relatively complex system, as a function of temperature and oxygen partial pressure; this will indicate the expected working conditions required to reach high methane conversion without the formation of unwanted products (CO_2 or H_2O). An ideal condition may be calculated for equilibrium conditions in the gas phase, as follows:

$$p\mathrm{CO}(p\mathrm{H_2})^2 = K_1\{(p\mathrm{O_2})^{1/2} p\mathrm{CH_4}\} \quad (4)$$

$$p\mathrm{CO_2} = K_2\{(p\mathrm{O_2})^{1/2} p\mathrm{CO}\} \quad (5)$$

$$p\mathrm{H_2O} = K_3\{(p\mathrm{O_2})^{1/2} p\mathrm{H_2}\} \quad (6)$$

where p_i denotes the partial pressure of species (atm). The Gibbs free energies ΔG_1, ΔG_2, and ΔG_3 were calculated from standard thermodynamic data, and used to obtain the corresponding values for equilibrium constants K_1, K_2 and K_3.

The gas composition will thus vary with the oxygen partial pressure (at constant temperature), and one still needs two additional conditions to estimate the gas composition for a given value of oxygen partial pressure. Such conditions can be obtained by taking into account the H:C = 4 ratio in methane, or

$$p\mathrm{H_2} + p\mathrm{H_2O} = 2(p\mathrm{CO} + p\mathrm{CO_2}). \quad (7)$$

In addition, the sum of the fractions of the different gases should be unit, i.e.

$$p\mathrm{H_2} + p\mathrm{H_2O} + p\mathrm{CO} + p\mathrm{CO_2} + p\mathrm{CH_4} = 1 \quad (8)$$

A solution for this problem can be obtained on combining Eqs. (5)–(8) to express the fractions of CO, H_2, CO_2, and H_2O as functions of the fraction of methane and partial pressure of oxygen as follows:

$$p\mathrm{CO} = \frac{(1/3)(1 - p\mathrm{CH_4})}{1 + K_2(p\mathrm{O_2})^{1/2}} \quad (9)$$

$$p\mathrm{H_2} = \frac{(2/3)(1 - p\mathrm{CH_4})}{1 + K_3(p\mathrm{O_2})^{1/2}} \quad (10)$$

$$p\mathrm{CO_2} = \frac{(1/3)(1 - p\mathrm{CH_4})}{1 + [K_2(p\mathrm{O_2})^{1/2}]^{-1}} \quad (11)$$

$$p\mathrm{H_2O} = \frac{(2/3)(1 - p\mathrm{CH_4})}{1 + [K_3(p\mathrm{O_2})^{1/2}]^{-1}} \quad (12)$$

Substitution of Eqs. (9) and (10) in Eq. (5) thus yields the dependence of partial pressure of methane on the oxygen partial pressure:

$$\frac{(1 - p\mathrm{CH_4})^3}{p\mathrm{CH_4}} = \tfrac{27}{4} K_1(p\mathrm{O_2})^{1/2}[1 + K_2(p\mathrm{O_2})^{1/2}] \times [1 + K_3(p\mathrm{O_2})^{1/2}]^2 \quad (13)$$

The dependence of pO_2 on [CH_4] was solved numerically (for given values of pCH_4), and the corresponding solution was replaced in Eqs. (9)–(12) to obtain the partial pressures of the remaining components of the gas mixture. Fig. 1 shows calculations for a typical temperature $T = 1173$ K.

3. Combined partial oxidation and water vapor reforming of methane

One may also attempt to design membranes for a combination of partial oxidation and water vapor reforming in mixed conducting membrane reactors. Such an approach should have advantages in what concerns the decrease in oxygen flux requirements, increasing the H_2:CO ratio, and also in terms of rendering the gas input less reducing, and

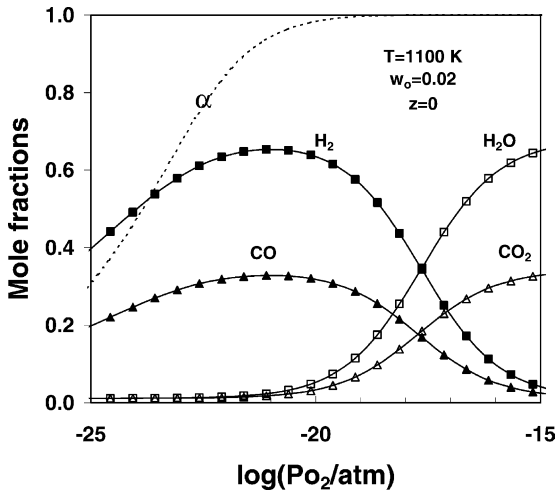

Fig. 1. Equilibrium gas composition and methane conversion as a function of oxygen partial pressure, at 1100 K, for steam:methane ratio 0.02.

thus less aggressive towards the mixed conducting membrane materials. Under equilibrium, steam reforming should be given by

$$CH_4 + H_2O \Leftrightarrow CO + 3H_2 \tag{14}$$

which corresponds to a combination of reactions 1 and 3.

Thus, one might still combine Eqs. (4)–(6) and (8). However, C:H ratio will be dependent on the water vapor content, which invalidates Eq. (7). Alternatively, the quantities of the different gas species can be expressed as a function of the fraction converted. One may thus derive those relations for 1 mole of methane in the input with the corresponding values of steam to methane ratio $w_0 = H_2O{:}CH_4$, and an inert to methane ratio z. On converting a fraction α of methane one obtains $1-\alpha$ moles of methane, α moles of $CO + CO_2$, $w_0 + 2\alpha$ moles of $H_2 + H_2O$, and the original quantity z of inert. From these quantities one easily obtains the following relations for the gas composition:

$$pCH_4 = \frac{1-\alpha}{1+z+w_0+2\alpha} \tag{15}$$

$$pCO + pCO_2 = \frac{\alpha}{1+z+w_0+2\alpha} \tag{16}$$

$$pH_2 + pH_2O = \frac{w_0+2\alpha}{1+z+w_0+2\alpha} \tag{17}$$

On combining Eq. (5) with Eq. (16), and Eq. (6) with Eq. (17) one thus obtains:

$$pCO = \frac{\alpha/(1+z+w_0+2\alpha)}{1+K_2(pO_2)^{1/2}} \tag{18}$$

$$pH_2 = \frac{(w_0+2\alpha)/(1+z+w_0+2\alpha)}{1+K_3(pO_2)^{1/2}} \tag{19}$$

$$pCO_2 = \frac{\alpha/(1+z+w_0+2\alpha)}{1+[K_2(pO_2)^{1/2}]^{-1}} \tag{20}$$

$$pH_2O = \frac{(w_0+2\alpha)/(1+z+w_0+2\alpha)}{1+[K_3(pO_2)^{1/2}]^{-1}} \tag{21}$$

On replacing Eqs. (14), (18) and (19) in Eq. (4) one finds the additional solution required to obtain the value of pO_2 for the assumed fraction reacted

$$\frac{(w_0+2\alpha)^2\alpha}{(1+z+w_0+2\alpha)^2(1-\alpha)} = K_1(pO_2)^{1/2}[1+K_2(pO_2)^{1/2}][1+K_3(pO_2)^{1/2}]^2 \tag{22}$$

A Fibonacci method [23] was then used to obtain the solutions of fraction reacted α for pre-selected values of oxygen partial pressure. The values of α and pO_2 were then inserted in Eqs. (18)–(21) to obtain the gas composition. The examples presented below were computed using the following equilibrium constants $K_i = \exp[-\Delta G_i/(RT)]$ extracted from thermodynamic data (e.g. [24])

$$K_1 = 14.6 \exp\frac{5.12\times10^3 + 6.17\log(T)}{T} \tag{23}$$

$$K_2 = 2.92\times10^{-5}\exp\frac{3.40\times10^4}{T} \tag{24}$$

$$K_3 = 1.37\times10^{-3}\exp\frac{2.96\times10^4}{T} \tag{25}$$

Typical examples are shown in Figs. 1 and 2, for methane with relatively low humidity ($w_0 = 0.02$), and for a mixture with water to methane ratio $w_0 = 0.25$. The predictions show a slight enrichment of hydrogen in the syngas, which may contribute to increase the efficiency. In addition, Fig. 3 shows a shift towards slightly less reducing conditions, for identical values of methane conversion, which corresponds to somewhat less severe working conditions. However, this

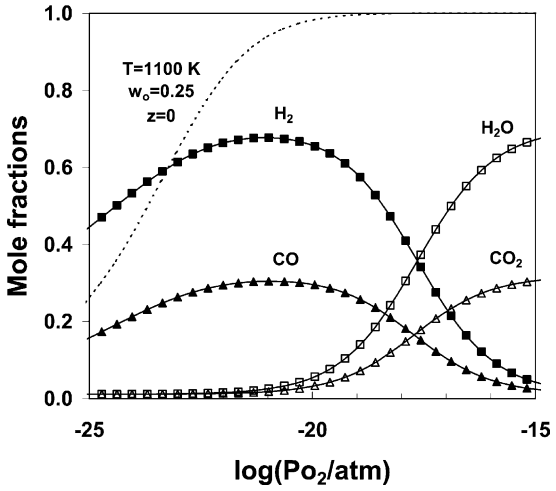

Fig. 2. Equilibrium gas composition and methane conversion as a function of oxygen partial pressure, at 1100 K, for steam:methane ratio 0.25. The dashed line represents the fraction converted, and the symbols represent the mole fractions of H_2 (■), CO (▲), CO_2 (△), and H_2O (□).

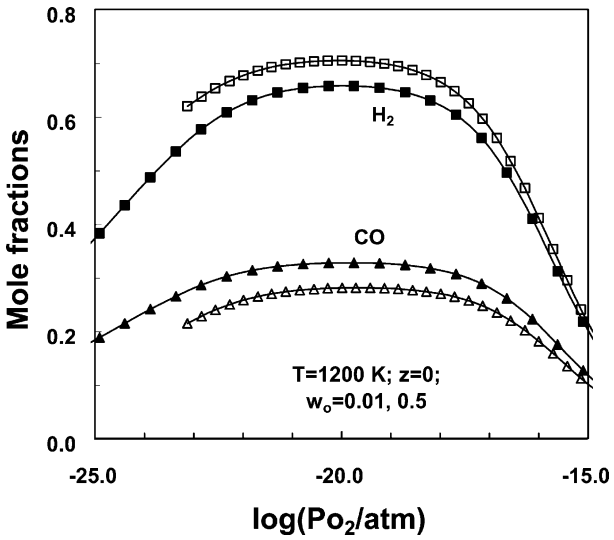

Fig. 3. Dependence of the fractions of H_2 (■, □) and CO (▲, △) vs. oxygen partial at 1200 K, with $z = 0$, and steam:methane ratio $w_0 = 0.01$ (closed symbols) and 0.5 (open symbols).

effect is negligible for nearly complete methane conversion. Though the fractions of different gas species are not shown in Fig. 3, these can be calculated by taking into account Eq. (18)–(21), with the relevant equilibrium constants (Eq. (23)–(25)). Similar calculations are shown in Fig. 4, for methane diluted with an inert gas, and wet.

4. Ideal solutions for tubular reactors

In the concept of mixed conducting membrane reactors the gas composition will be dependent on the permeability of those membranes, and reactor configuration. For continuous reactors one might assume typical chemical engineering concepts such as the continuous tubular reactor, and the continuous stirred reactor. In this section one considers a tubular concept, with a mixed conducting membrane of internal diameter D, and thickness $h \ll D$ (Fig. 5). The oxygen permeation rate (moles per unit area and per unit time) across the walls of mixed conducting membrane is

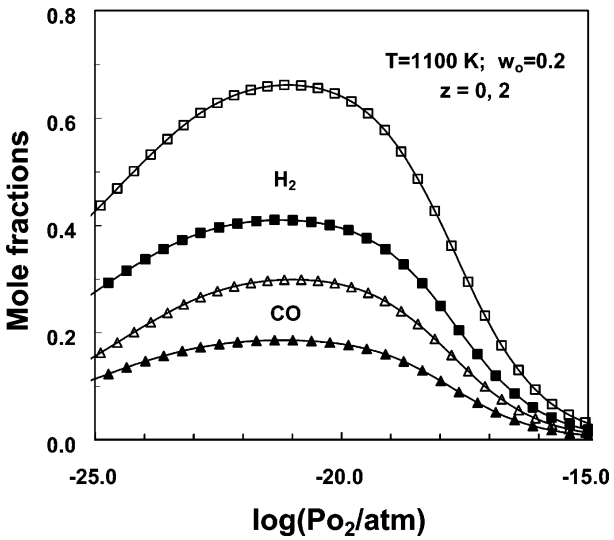

Fig. 4. Dependence of the fraction of H_2 (■, □) and CO (▲, △) as a function of oxygen partial pressure, at 1100 K, for a steam:methane ratio ($w_0 = 0.2$), and for inert:methane ratio $z = 0$ (△, □) and 2 (▲, ■).

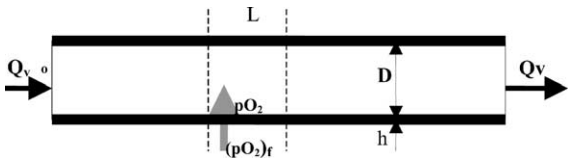

Fig. 5. Schematic representation of a tubular mixed conducting membrane reaction.

$$jO_2 = \frac{JO_2 \ln\{(pO_2)_f / pO_2\}}{h} \tag{26}$$

where JO_2 is the specific oxygen permeability of the selected membrane material and h is the membrane wall thickness. The oxygen partial pressure in the feed side of the membrane where $(pO_2)_f$ is typically 0.21 atm, in air.

A molar balance to oxygen may be expressed on selecting an element of length δL, and writing the input and output of all oxidized species as follows:

$$2\left\{\frac{JO_2 \ln[(pO_2)_f / pO_2]}{h}\right\} \pi D\, \delta L = C_T Q_V^0\, \delta Y_0 \tag{27}$$

where C_T is total gas concentration, Q_V^0 the input volume flow rate entering the tubular reactor, and

$$Y = \left(\frac{Q_V}{Q_V^0}\right)(pH_2O + pCO + 2pCO_2) \tag{28}$$

This is a weighted contribution of all oxygen containing species after accounting for the expected volume expansion, i.e. $Q_V > Q_V^0$. Though oxidized species might also diffuse up-stream, and reduced species down-stream, one assumed that these effects are negligible when compared to the oxidation process, and to the flow rate in the longitudinal direction. This may not be the case when diffusion is relatively fast, and/or the oxidation is slow, thus requiring low flow rates.

Volume expansion can be described by recalling the relevant relations between the contents of different gas species and the fraction converted, shown above. These relations yield

$$\frac{Q_V}{Q_V^0} = \frac{1 + 2\alpha + z + w_0}{1 + z + w_0} \tag{29}$$

and on replacing this in Eqs. (18), (20), (21) and (29) in Eq. (28) one obtains

$$Y = (1 + z + w_0)^{-1}\{(w_0 + 2\alpha)(1 + K_3^{-1} pO_2^{-1/2})^{-1} + \alpha + \alpha(1 + K_2^{-1} pO_2^{-1/2})^{-1}\} \tag{30}$$

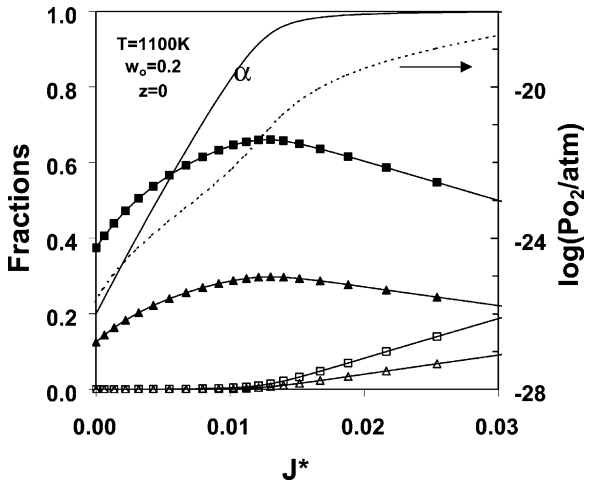

Fig. 6. Simulation of the dependence of methane conversion (—), gas composition (symbols), and oxygen partial pressure (- - -) as a function of dimensionless permeability, for a tubular reactor concept. The symbols represent the mole fractions of H_2 (■), CO (▲), CO_2 (△), and H_2O (□).

Therefore, the values of Y can be related to previously computed sets of results for the fraction of methane converted, and the corresponding values of oxygen partial pressure. Thus, Eq. (27) can be rearranged as follows:

$$\frac{\pi DL\, JO_2}{hQ_V^0 C_T} = 0.5 \int_{Y_{in}}^{Y_{out}} \ln\left[\frac{(pO_2)_f}{pO_2}\right]^{-1} dY \tag{31}$$

and solved to obtain the conditions required to attain the desired conversion. The value of Y at the entry of the tubular reactor reduces to

$$Y_{in} = \frac{w_0}{1 + z + w_0} \tag{32}$$

Actually, these calculations were based on previous calculations of the dependence of fraction reacted and gas on oxygen partial pressure, for a series of values of pO_2, thus yielding sets of $(pO_2)_k$, α_k, $k = 0, 1, 2, 3, \ldots$, and the corresponding values of Y_k. A Runge–Kutta method [25] was then used to perform the integration of Eq. (30).

An example of these calculations is shown in Fig. 6, for wet methane with $w_0 = 0.2$. These results show the dependence of gas composition on the dimensionless permeability

$$J^* = \frac{JO_2 \pi DL}{hC_T Q_V^0} = \frac{JO_2\, A}{hC_T Q_V^0} \tag{33}$$

A being the exchange area of the tubular reactor. The dimensionless permeability accounts for the combined effects of the membrane permeability, thickness, other geometrical characteristics of the tubular reactor (diameter and length), and flow rate. For example, a membrane material with insufficient permeability requires either thinner membranes, or lower flow rates to attain the required conversion. Otherwise, one needs tubular reactors with longer length or larger diameter. Note also that the representation shown in Fig. 6, also corresponds to the changes in composition and oxygen

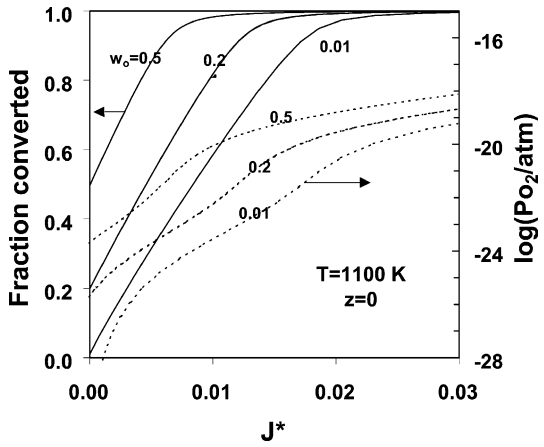

Fig. 7. Simulation of the dependence of methane conversion (—), and oxygen partial pressure (- - -) as a function of dimensionless permeability, at 1100 K, and for different values of the steam:methane ratio ($w_0 = 0.01$, 0.2, 0.5).

partial pressure along the length of the tubular reactor, for given values of the membrane diameters and thickness, and for flow rate.

The effects of water vapor partial pressure at the entry of the tubular reactor are shown in Fig. 7, and effects of dilution of methane with an inert gas are shown in Fig. 8. These calculations show that one might rely on membrane materials with lower permeability, or use a lower membrane area to attain a given fraction converted by promoting simultaneous steam reforming.

Eq. (31) may also be rewritten to describe the changes of oxygen chemical potential at a generic distance from the entry, along the length of a tubular reactor, and for a given conditions of membrane permeability, membrane diameter and total length, and volume flow rate at the input, i.e. for a given value of dimensionless permeability $J^* =$

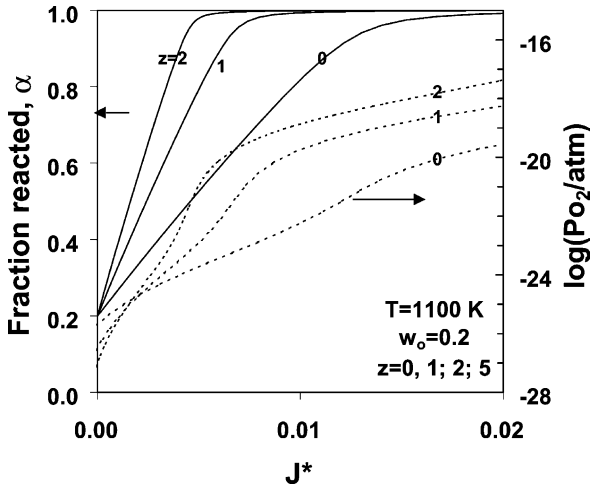

Fig. 8. Simulation of the dependence of methane conversion (—), and oxygen partial pressure (- - -) as a function of dimensionless permeability, at 1100 K, for $w_0 = 0.2$, and with different values of inert:methane ratio $z = 0$, 1, and 2.

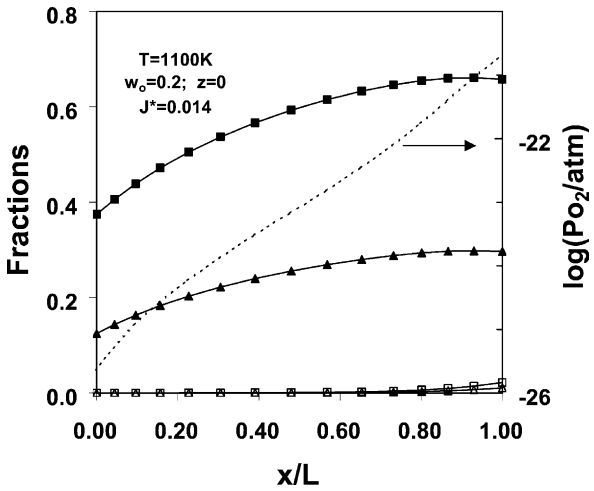

Fig. 9. Simulation of the evolution of gas composition (symbols), and oxygen partial pressure (---), along the length of a tubular membrane reactor with a dimensionless permeability $J^* = 0.014$. The symbols represent the mole fractions of H_2 (■), CO (▲), CO_2 (△), and H_2O (□).

$\pi DL\, JO_2/hQ_V^0 C_T$. In this case

$$\frac{x}{L} = (2J^*)^{-1} \int_{Y_{in}}^{Y} \ln\left[\frac{(pO_2)_f}{pO_2}\right]^{-1} dY' \tag{34}$$

A typical example is shown in Fig. 9, to emphasize that the membrane materials are more likely to undergo degradation under severe reducing conditions near the input. One should thus rely mainly on steam reforming near the entry, by resorting to suitable catalysts supported on materials with enhanced stability.

The predictions shown in Figs. 6–9 are probably unrealistic, at least at the entry. In fact, it is assumed that steam reforming occurs instantaneously on entering the tubular reactor. The effects of kinetic limitations are being simulated, and will be dealt with in a separate report.

5. Model for CSTR reactors

A simpler balance can be derived on assuming a perfectly stirred continuous reactor, with volume V, with a volume flow rate Q_V^0 at the entry, and an area A of mixed conducting wall for the supply of oxygen. In this case, the relevant balance of oxygen reduces to

$$2A\left\{\frac{JO_2 \ln[(pO_2)_f/pO_2]}{h}\right\} = C_T Q_V\{pH_2O + pCO + 2pCO_2\} - C_T Q_V^0\{(pH_2O)_0 + (pCO)_0 + 2(pCO_2)_0\} \tag{35}$$

This can be combined with Eqs. (18), (20) and (21) and re-arranged to obtain the following generic

$$\frac{JO_2 A}{hQ_V^0 C_T} = 0.5 \ln\left[\frac{(pO_2)_f}{pO_2}\right]^{-1} (Y_{out} - Y_{in}) \tag{36}$$

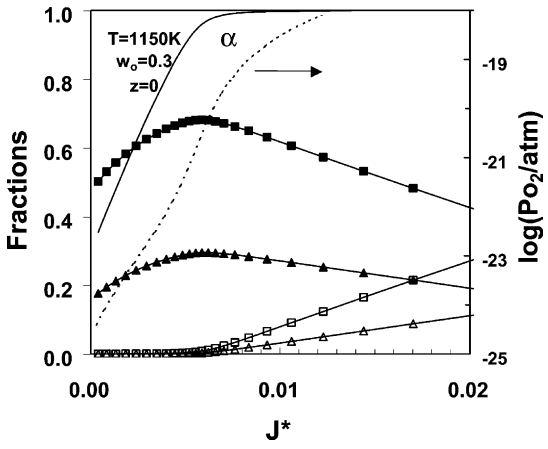

Fig. 10. Predictions of methane conversion, gas composition and oxygen partial pressure on dimensionless permeability, for a CSTR reactor concept. The symbols represent the mole fractions of H_2 (■), CO (▲), CO_2 (△), and H_2O (□).

Eq. (30) can be used to obtain the value of Y_{out} for the required conversion, and $Y_{in} = w_0/(1 + z + w_0)$.

Eq. (36) can thus be used to describe the dependence of fraction crystallized on the permeability of the membrane material, geometric characteristics of the reactor, and flow rate, all included in the dimensionless permeability:

$$J^* = \frac{JO_2\, A}{hC_T\, Q_V^0} \tag{37}$$

Thus, the dependence of fraction reacted on the permeability is easily obtained by inserting the previously computed dependence of fraction reacted on the oxygen partial pressure. One typical example is shown in Fig. 10. Though this CSTR concept is less sensitive to a very reducing input, it is very likely to require much larger volume to area ratios, and thus lower efficiency for partial oxidation.

6. Stability requirements of membrane materials

Figs. 1–4 show that the highest values of the fractions of H_2 and CO are attained for pO_2 close to 10^{-21} atm, at 1100 K. The corresponding conversion of methane is already in the order of 95%. On shifting the operating conditions to more oxidizing one may thus expect the onset of completely oxidized species (i.e. CO_2 and H_2O). The conditions required to attain the highest yield of H_2 and CO are slightly temperature dependent (dashed-dotted line in Fig. 11), whereas effects of humidity (Fig. 3) and of dilution with an inert gas (Fig. 4) are relatively weak.

The results shown in Fig. 11 are also a guideline for assessing the stability requirements of mixed conducting membrane materials. Note that known mixed conductors have limited stability under reducing conditions. Typical examples are materials with perovskite or related structure types, such as $LaCoO_3$ or $LaFeO_3$, with partial substitution

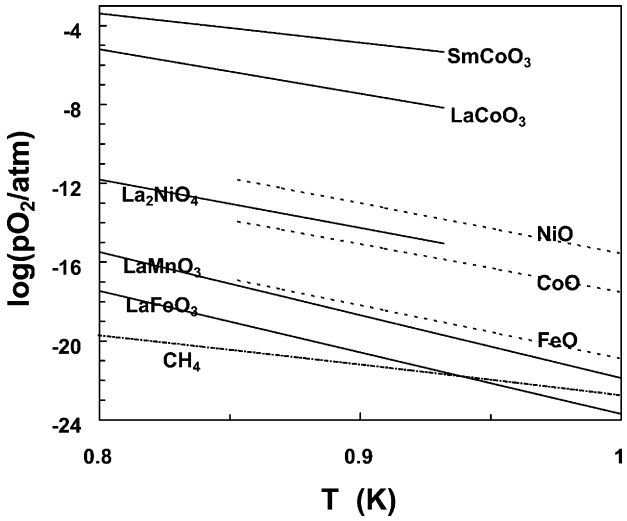

Fig. 11. Predictions of conditions required to obtain the highest yield of H_2 and CO by partial oxidation of methane with steam:methane ratio $w_0 = 0.25$ (-···-), and typical stability limits of prospective mixed conductors, and stability of other oxides (NiO, CoO and FeO) added to mixed conductors based on lanthanum gallate or titanates.

of Ln^{3+} by Sr^{2+}, and La_2NiO_4. Their stability ranges were thus assessed using results reported in the literature [26–29], and are compared to the expected working conditions required for the conversion of methane. These results suggest that one should seek candidate materials based on $LaFeO_3$ and possibly also $LaMnO_3$ with suitable composition changes, to enhance the transport properties. For example, $(La,Sr)FeO_{3-\delta}$ might be candidate materials with a compromise between permeability and stability. Other promising mixed conductors are based on lanthanum gallate [14,15] or titanates [11–13] with additions of Ni, Co or Fe. In these cases, the stability limitations are probably determined mainly by the reducibility of the additives. The stability limits of single oxides (e.g. NiO, CoO and FeO) were thus computed from thermodynamic data, and are shown as guidelines for materials containing these oxides.

7. Conclusions

A combination of analytical and numerical methods can be used to describe the processes of partial oxidation and steam reforming of methane, under equilibrium conditions, and as a function of oxygen partial pressure. This dependence of fraction of methane converted and the corresponding fractions of CO, H_2O and CO_2 can be used to derive solutions for the steady state regimes in typical tubular reactor and CSTR reactor concepts with mixed conducting walls. A single dimensionless parameter may account for the combined effects of oxygen permeability of the reactor wall, geometric characteristics and volume flow rate. Selected examples showed that partial steam reforming may be crucial to avoid excessively reducing conditions at the entry, and to protect the mixed conducting membrane materials exposed to those conditions. Slow surface exchange also causes a gradient of chemical potential at the permeate side of the membrane, and might contribute to bridge the gap between the stability limits of membrane materials and excessively reducing conditions inside the reactor.

Acknowledgements

Work supported by the NATO SfP978002 and INTAS 00276 projects.

References

[1] H.J.M. Bouwmeester, A.J. Burgraaf, Dense ceramic membranes for oxygen separation, in: A.J. Burgraaf, L. Cot (Eds.), Fundamentals of Inorganic Membrane Science and Technology, Elsevier, Amsterdam, 1996, p. 435.
[2] V.V. Kharton, A.A. Yaremchenko, A.V. Kovalevsky, A.P. Viskup, E.N. Naumovich, P.F. Kerko, J. Memb. Sci. 163 (1999) 307.
[3] T.J. Mazanec, T.L. Cable, J.G. Frye, W.R. Kliewer, US Patent 5,591,315 (1997), assigned to Standard Oil Company.
[4] M. Schwartz, J.H. White, A.F. Sammells, Int. Patent Application PCT WO 97/41060 (1996), assigned to Eltron Research, Inc.
[5] Y. Shen, A.V. Joshi, K. Krist, M. Liu, A.V. Virkar, US Patent 5,616,223 (1997), assigned to Gas Research Institute.
[6] B. Vigeland, R. Glenne, T. Breivik, S. Julsrud, Int. Patent Application PCT WO 99/59702 (1999), assigned to Norsk Hydro ASA.
[7] R.M. Thorogood, R. Srinivasan, T.F. Yee, M.P. Drake, US Patent 5,240,480 (1993), assigned to Air Products and Chemicals, Inc.
[8] U. Balachandran, M. Kleefisch, T.P. Kobylinsky, S.L. Morissette, S. Pei, Int. Patent Application PCT WO 94/24065 (1994), assigned to Amoco Corp.
[9] H. Iwahara, T. Esaka, T. Mangahara, J. Appl. Electrochem. 18 (1988) 173.
[10] V.V. Galvita, V.D. Belyaev, A.K. Demin, V.A. Sobyanin, Appl. Catal. A: Gen. 165 (1997) 301.
[11] J.R. Jurado, F.M. Figueiredo, B. Gharbage, J.R. Frade, Solid State Ion. 118 (1999) 89.
[12] V.V. Kharton, A.V. Kovalevsky, E.V. Tsipis, A.P. Viskup, E.N. Naumovich, J.R. Jurado, J.R. Frade, J. Solid State Electrochem. 7 (2002) 30.
[13] F.M. Figueiredo, J. Waerenborgh, V.V. Kharton, H. Naefe, J.R. Frade, Solid State Ion. 156 (2003) 371.
[14] V.V. Kharton, A.P. Viskup, A.A. Yaremchenko, R.T. Baker, B. Gharbage, G.C. Mather, F.M. Figueiredo, E.N. Naumovich, F.M.B. Marques, Solid State Ion. 132 (2000) 119.
[15] I.A. Leonidov, V.L. Kozhevnikov, E.B. Mitberg, M.V. Patrakeev, V.V. Kharton, F.M.B. Marques, J. Mater. Chem. 11 (2001) 1202.
[16] Q. Ming, M.D. Nersesyan, A. Wagner, J. Ritchie, J.T. Richardson, D. Luss, A.J. Jacobson, Y.L. Yang, Solid State Ion. 122 (1999) 113.
[17] V.V. Kharton, A.P. Viskup, E.N. Naumovich, F.M.B. Marques, J. Mater. Chem. 9 (1999) 2623.
[18] V.V. Kharton, A.P. Viskup, A.V. Kovalevsky, E.N. Naumovich, F.M.B. Marques, Solid State Ion. 143 (2001) 337.
[19] A.A. Yaremchenko, V.V. Kharton, M.V. Patrakeev, J.R. Frade, J. Mater. Chem. 13 (2003) 1136.
[20] P. Vernoux, J. Guindet, M. Kleitz, J. Electrochem. Soc. 145 (1998) 3487.

[21] E.S. Putna, J. Stubenrauch, J.M. Vohs, R.J. Gorte, Langmuir 11 (1995) 4832–4837.
[22] S. Park, J.M. Vohs, R.J. Gorte, Nature 404 (2000) 265.
[23] G. Beveridge, R. Schechter, Optimisation, Theory and Practice, McGraw-Hill, 1970.
[24] J.A. Dean (Ed.), Lange's Handbook of Chemistry, 12th ed., McGraw Hill, 1979, New York.
[25] R.L. Burden, J.D. Faires, A.C. Reynolds, Numerical Analysis, 12th ed., Prindle, Weber and Schimdt, 1978.
[26] V.A. Cherepanov, A.N. Petrov, L.Y. Grimova, E.M. Novitskii, Zh. Fiz. Khim. 57 (1983) 859–863.
[27] A.N. Petrov, V.A. Cherepanov, A.Y. Zuev, Zh. Fiz. Khim. 61 (1987) 630.
[28] A.Y. Kropanov, A.N. Petrov, V.M. Zhukovsky, Zh. Neorg. Khim. 28 (1983) 2938.
[29] T. Nakamura, G. Petzov, L.J. Gaukler, Mater. Res. Bull. 15 (1979) 649.